

Gallium-rich reconstructions on GaAs(001)

M. Pristovsek^{*,1}, S. Tsukamoto^{**,1}, A. Ohtake¹, N. Koguchi¹, B. G. Orr²,
W. G. Schmidt³, and J. Bernholc³

¹ Nano-Device Research Group, National Institute for Materials Science, Sengen 1-2-1 Tsukuba, Ibaraki 305-0047, Japan

² Randall Laboratory of Physics, The University of Michigan, 500 E. University, Ann Arbor, Michigan 48109-1120, USA.

³ Department of Physics, North Carolina State University, Raleigh, North Carolina 27695-8202, USA

Received 14 May 2003, revised 9 July 2003, accepted 5 August 2003

Published online 6 October 2003

PACS 61.14.Hg; 68.35.Bs; 78.66.Fd; 81.15.Hi

Ga-rich reconstructions on GaAs(001) surfaces were prepared by annealing and Ga dosing of Molecular Beam Epitaxy grown samples and analyzed *in-situ* by Reflectance Anisotropy Spectroscopy and Reflection High-Energy Electron Diffraction. Annealing or dosing gallium above about 800 K invariably results in a $(4 \times 2)/c(8 \times 2)$ reconstruction. Lowering the temperature or annealing below 800 K results in a $(2 \times 6)/(3 \times 6)$ reconstruction. By dosing the $(2 \times 6)/(3 \times 6)$ reconstruction with more than 0.2 monolayer of gallium, it transforms into a (4×6) reconstruction. The observed translational symmetries and measured RAS spectra are compared with results of *first-principles* calculations. None of the (2×6) structures proposed in the literature is energetically stable. The RAS spectrum calculated for the $\zeta(4 \times 2)$ model resembles reasonably the data measured for the (4×2) surface. The RAS spectra calculated for (2×6) symmetries indicate that mixed Ga-As dimers likely are a structural element of the corresponding surface reconstructions.

© 2003 WILEY-VCH Verlag GmbH & Co. KGaA, Weinheim

1 Introduction

Gallium-rich surfaces on GaAs(001) have been investigated for a long time by both experiment [1–16] and theory [15–20]. Nevertheless, their microscopic structure is far from being understood. In particular, the $c(8 \times 2)/(4 \times 2)$ reconstruction is still a topic of recent discussion [13, 15, 21, 22]. This reconstruction often appears in conjunction with $n \times 6$ symmetries along [110] [4, 12, 22]. The atomic structures giving rise to these six-fold periodicities are not known.

The aim of this study is to clarify the preparation conditions which lead to the appearance of these Ga-rich GaAs surface structures, especially to those with six-fold symmetries, and to contribute to their microscopic understanding. To this end we combine *in-situ* Reflection High-Energy Electron Diffraction (RHEED) for symmetry and *in-situ* Reflectance Anisotropy Spectroscopy (RAS) for surface structure information. The experimental findings are compared with surface energies and RAS spectra calculated from *first principles*.

* Corresponding author: e-mail: prissi@physik.tu-berlin.de,

present address: Ferdinand-Braun-Institut für Höchstfrequenztechnik, Albert-Einstein-Str. 11, 12489 Berlin, Germany, Phone: +49 30 6392 2672, Fax: +49 30 6392 2685

** Present address: The University of Tokyo, Institute for Industrial Science, 4-6-1 Komaba Meguro-Ku, Tokyo 153-8505, Japan

© 2003 WILEY-VCH Verlag GmbH & Co. KGaA, Weinheim

2 Experimental

The experiments were performed in a Molecular Beam Epitaxy (MBE) chamber with a base pressure around 10^{-8} Pa. As₄ and Ga were the sources for buffer growth. We use doped and undoped GaAs (001) either singular or 1° off vicinal. The RAS measurements were made through a strain reduced viewport with a modified JobinYvon RDS spectrometer. The RHEED images were recorded at 30 kV using a Canon PowerShot G2 Digital camera. The sample temperature was calibrated by a side-on pyrometer.

Prior to the experiments we tried to minimize the arsenic background pressure in the MBE chamber. For that the samples were capped with an amorphous arsenic layer after buffer growth and transferred into a neighboring chamber ($p = 5 \times 10^{-9}$ Pa). Then the heater in the MBE chamber was set to 850 K until the total pressure was about 5×10^{-8} Pa (without liquid nitrogen in the cryo-shroud). By this procedure and using the cryo-shroud, the background pressure was in the mid 10^{-8} Pa range, even with the sample at 825 K, while direct annealing at 825 K results in a background pressure in the mid 10^{-7} Pa range. However, we found no difference compared to the results obtained from samples which were directly annealed after growth. After decapping or growth, the initial surface prior to the high-temperature annealing was always reconstructed $c(4 \times 4)$. Quenching of the samples was done by quickly removing the samples at 850 K from the heated substrate holder and move them between the cryo-shroud. This procedure usually takes less than 5 seconds. The samples holder were very small, only 2.5 cm², and hollow directly behind the actual sample. Thus cooling rates using quenching are about 100 K/s.

3 Computational

The calculations are based on a massively parallel real-space multigrid implementation [23] of the density-functional theory in the local-density approximation (DFT-LDA). We model the surface by a periodic arrangement of asymmetric slabs consisting of 12 GaAs layers, separated by 8 layers of vacuum. The dangling bonds at the bottom layer of the slab are saturated by pseudohydrogen ($Z = 1.25$). Further details of the calculations are like those in Ref. [19]. Based on the electronic structure obtained within DFT-LDA, we calculate the reflectance anisotropy in the independent-particle approximation following Del Sole [24] and Manghi et al. [25]. Optical spectra are usually strongly influenced by many-body effects such as self-energy corrections and electron-hole attraction [26]. In the case of RAS, however, some error cancellation occurs: RAS spectra are difference spectra, normalized to the bulk dielectric function (cf. Eq. 10 in Ref. [25]). Therefore, single-particle calculations within DFT-LDA are usually reliable in predicting surface optical anisotropies [27]. Accordingly, we simply use the scissors-operator approach [28] with an energy shift of 0.6 eV to take self-energy effects into account. The wave-vector and energy dependence of the quasiparticle corrections as well as excitonic and local-field effects are neglected. Furthermore, spin-orbit coupling – which leads to additional structures in the experimental spectra, in particular at the energies of the bulk critical point energies – is not contained in our calculations.

In order to model GaAs(001) surfaces with a $\times 6$ symmetry along [110] we considered a series of structures shown in Fig. 1. Due to computer memory limitations, our calculations are limited to (2×6) unit mesh sizes. Therefore, larger surface structures proposed in the literature were approximated by (2×6) configurations that contained the respective structural elements as described in the following:

The probably first explanation for $\times 6$ periodicities goes back to the structural model for a (2×6) surface proposed by Biegelsen et al. [7]. The blocks of parallel As dimers characteristic for the (6×6) structure of Kuball et al. [29] are modeled by a modified (2×6) structure and the combination of As and Ga dimers proposed by McLean et al. [12] to explain the (6×6) GaAs surface is represented by the $\alpha(2 \times 6)$ structure in Fig. 1. Many III–V(001) semiconductor surfaces form hybrid anion-cation dimers for group-III rich preparation conditions [15, 20]. Therefore, we also investigated the stability

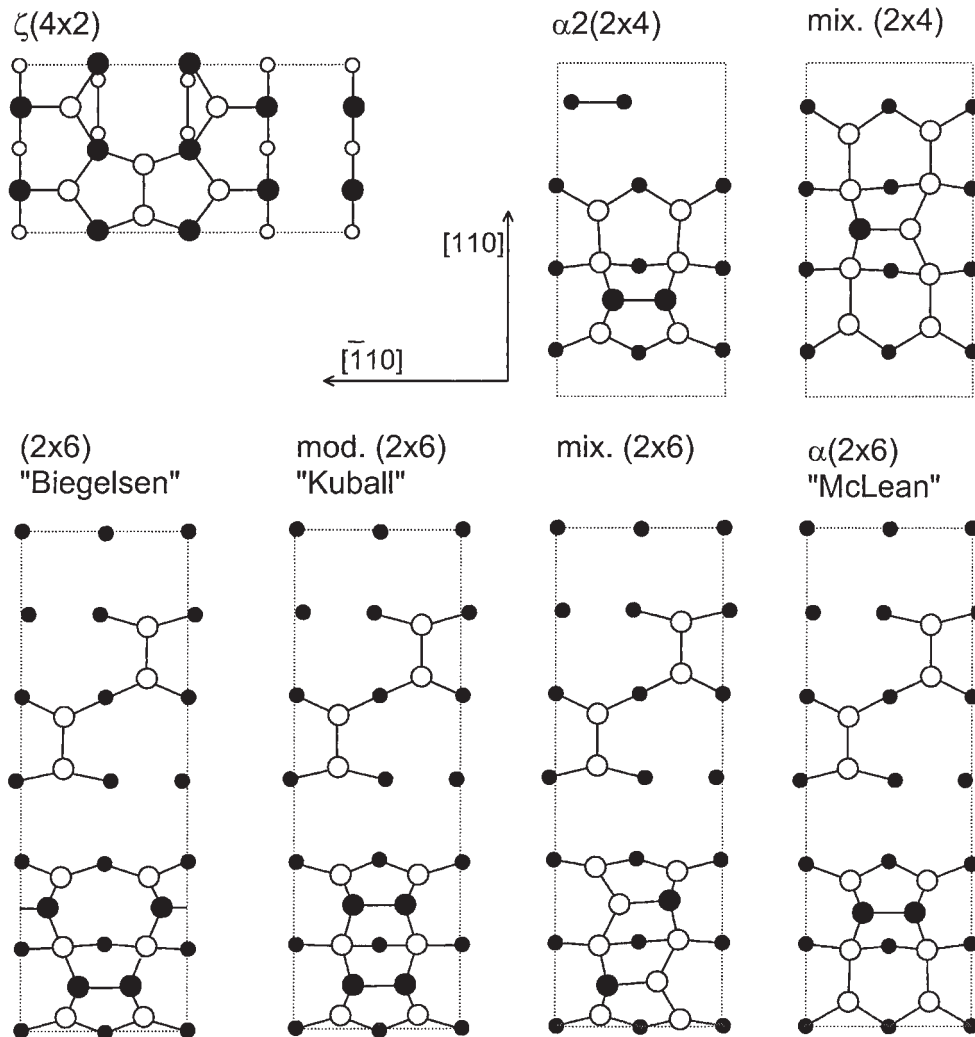


Fig. 1 Top view of relaxed GaAs(001) surface structures whose RAS spectra have been calculated. Empty (filled) circles represent Ga(As) atoms. Positions in the uppermost two atomic layers are indicated by larger symbols.

and optical fingerprints of mixed Ga-As dimers using the mixed (2×6) structure. For comparison, we include in our discussion of Ga-rich GaAs surfaces also the recently proposed $\zeta(4 \times 2)$ [14, 16, 18] surface and the $\alpha 2(2 \times 4)$ and mixed-dimer (2×4) geometries (cf. Fig. 1). These structures, as well as Biegelsens model for the (2×6) surface [7], have been subject to previous total-energy calculations by one of the present authors [19, 20].

4 Results and discussion

Table 1 summarizes the conditions to obtain the RHEED pattern of the three well-defined surfaces found in this study. Above 800 K, the surface always shows a $(4 \times 2)/c(8 \times 2)$ RHEED pattern (Fig. 2a). By dosing gallium, this surface roughens and the RHEED pattern becomes spotty and faint. The symmetry, however, does not change. By lowering the temperature or by annealing below 800 K, the surface develops a $(2 \times 6)/(3 \times 6)$ pattern (also called $(1 \times 6) + \frac{1}{6}nY^*$). This behavior has also

Table 1 Observed symmetries for different conditions, annealing without As (total pressure $< 10^{-7}$ Pa).

	Gallium dosing (monolayer)		
	+0 ML	+0.25 ML	> 3 ML
$T > 800$ K	(4×2)	(4×2)	spotty (4×1)
$T < 800$ K	fast $\uparrow\downarrow > 10$ min $(2 \times 6)/(3 \times 6)$	$\swarrow > 10$ min \uparrow fast \leftarrow 10 min (4×6)	$\uparrow\downarrow$ spotty (4×6)

been observed by others [1–4, 11, 12, 22]. The RHEED image of the $(2 \times 6)/(3 \times 6)$ in Fig. 2b clearly shows streaks at $\frac{1}{3}$, $\frac{1}{2}$, and $\frac{2}{3}$ along $[110]$. The intensity maximum of the twofold and threefold streaks is at different heights of the screen, which indicates separate domains. Therefore, the surface is best explained by a mixture of (2×6) and (3×6) reconstructed domains.

Only by quenching (i.e. fast removing the hot sample from the heater) a (4×2) RHEED pattern at room temperature can be obtained. Slower (i.e. more than 10 s) removal results in the appearance of a (4×6) pattern. The same pattern appears after annealing a quenched (4×2) above 500 K. Annealing this surface either at temperatures above 600 K or for a some time (longer than half an hour at $T > 500$ K) results again in a $(2 \times 6)/(3 \times 6)$ symmetry.

The change between $(2 \times 6)/(3 \times 6)$ and (4×2) symmetries is reversible, suggesting that the respective surface energies are similar. The transition to (4×2) happens almost instantaneously upon raising the temperature, while the reverse transition to $(2 \times 6)/(3 \times 6)$ takes much longer, about 10 min at 750 K. We can think of several causes for the reversible phase transition. The increase of the lattice constant with temperature may favor the (4×2) reconstruction at higher temperatures. For the InAs(001) surface the influence of strain on the relative stability of surface reconstructions has explicitly been shown [30]. Another possibility are different entropy contributions to the surface free energy $F = U - TS$ for finite temperatures. Entropy effects, while usually neglected, are not necessarily small [31]. Finally, the phase transition may be caused by changes of the surface stoichiometry, e.g. As desorption or segregation. In fact, Bayliss and Kirk [32] observed increased As desorption in ultra high vacuum simultaneously with the appearance of a (4×1) symmetry at temperatures around 750 K. Thermal Programmed Desorption (TPD) measurements on (4×6) surfaces [33, 34] found the onset of bulk arsenic desorption around 850 K. These findings, together with the different time constants for the $(2 \times 6)/(3 \times 6) - (4 \times 2)$ phase transition indicate that the last possibility may be the most likely explanation: When the temperature is increased, As desorbs from the $(2 \times 6)/(3 \times 6)$ and the surface transforms quickly into (4×2) . By lowering the temperature, excess arsenic from the bulk segregates slowly to the gallium rich (4×2) surface [35] and causes the transformation into a $(2 \times 6)/(3 \times 6)$ reconstructed surface.

By dosing a small amount of Ga (0.25–0.5 ML) at elevated temperature (550–800 K range), the $(2 \times 6)/(3 \times 6)$ reconstruction immediately transforms into a (4×6) structure. On this surface the main fourfold streaks along $[1\bar{1}0]$ are quite strong, but in the second Laue circle the fourfold symmetry is weaker, which might indicate a mixture of $1 \times$ and $4 \times$ symmetry (Fig. 2c). In the $[1\bar{1}0]$ azimuth sometimes a weak $\times 4$ symmetry is found, which corresponds to high temperature STM images of this surface [21]. This (4×6) surface occurs at extreme Ga-rich conditions. Ga droplets can be present on the (4×6) surface, especially after longer annealing time or higher amounts of gallium deposited, after the sample is cooled down.

Due to the varying surface stoichiometry, the calculated total energies of the GaAs surface structures cannot directly be used to determine the surface ground state. Rather, the thermodynamic grand-canonical potential Ω in dependence on the chemical potentials μ of Ga and As needs to be considered. Since the surface is in equilibrium with the bulk compound, $\mu(\text{Ga})$ and $\mu(\text{As})$ are related to each

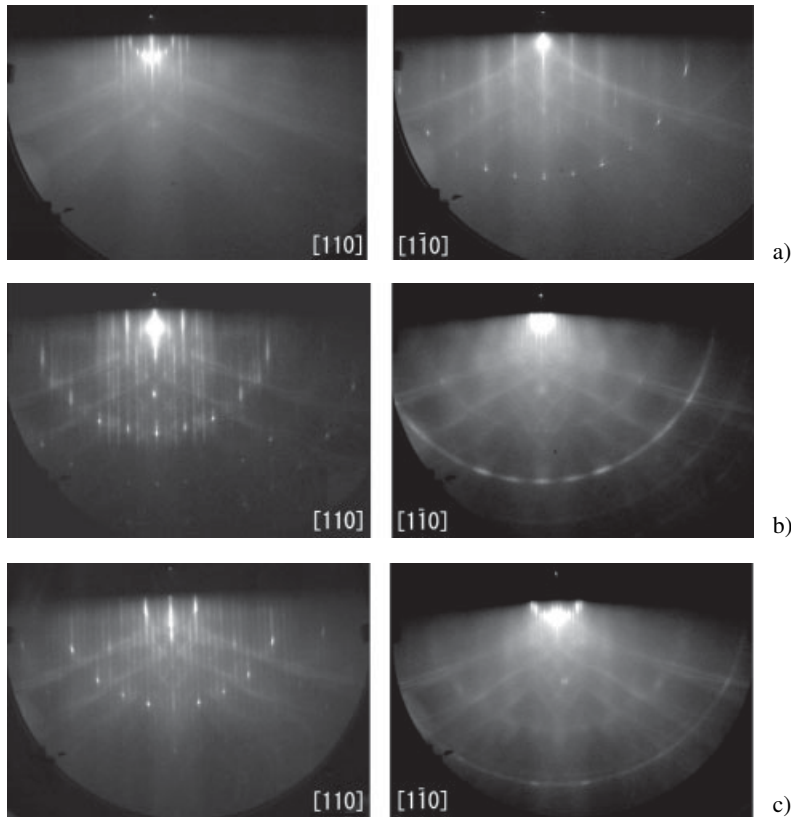


Fig. 2 RHEED images of the (4×2) (upper), $(2 \times 6)/(3 \times 6)$ (middle) and (4×6) (lower). The image of the (4×2) was taken at 825 K, the other ones at 300 K.

other. Their sum equals the chemical potential of bulk GaAs. Consequently, the surface formation energy may be written as a function of only one variable, which we take to be the relative chemical potential of the cation with respect to its bulk phase, $\Delta\mu(\text{Ga})$. Fig. 3 shows the resulting surface phase diagram for the structures explained in Fig. 1. For comparison, also the well-known As-rich $c(4 \times 4)$ and $\beta 2(2 \times 4)$ reconstructions have been included.

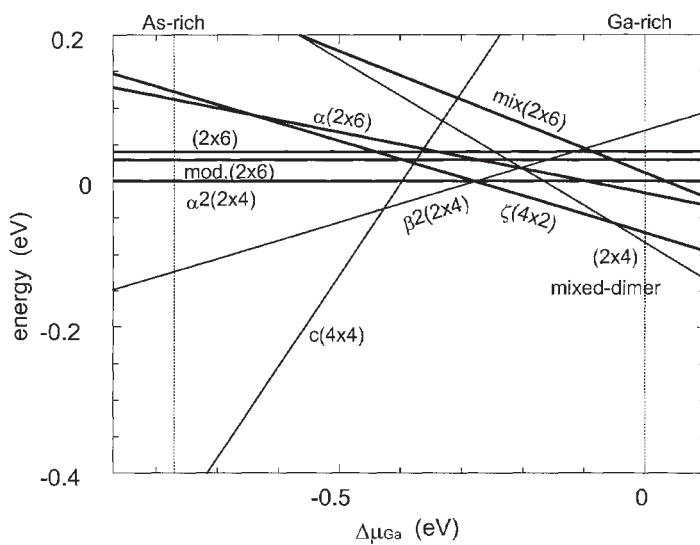


Fig. 3 Relative formation energy with respect to the $\alpha 2(2 \times 4)$ surface per (1×1) unit cell for GaAs surface reconstructions vs. the cation chemical potential at 0 K. For a given chemical potential $\Delta\mu(\text{Ga})$ the surface which has the lowest energy is the most stable surface at that condition. Dashed lines mark the approximate arsenic- and gallium-rich limits of the thermodynamically allowed range of $\Delta\mu(\text{Ga})$. Thick lines indicate surfaces which RAS spectra have been calculated in this paper.

The data in Fig. 3 implies that none of the (2×6) structures investigated here is a low-energy structure. In particular Biegelsen's model for the (2×6) symmetry [7] is unstable with respect to a block-like arrangement of As dimers as concluded from STM images by Kuball and co-workers [29]. Our total-energy results also question the structure proposed by McLean's et al. [12]. For Ga-rich surfaces, the recently proposed $\zeta(4 \times 2)$ surface is energetically most favored. Interestingly, the calculations indicate the appearance of (2×4) symmetries induced by mixed Ga-As dimers for extreme cation-rich preparation conditions. While this finding has been confirmed experimentally for InP and GaP(001) surfaces [15], no corresponding structure has ever been reported in an experimental study on GaAs.

Surface structure information and in particular hints for the occurrence of specific structural motifs can be obtained from RAS measurements. In Fig. 4 we present RAS spectra measured at room temperature after quenching the samples. These data are compared with DFT-LDA calculations. It should be noted that temperature effects, neglected in the calculations, considerably broaden and redshift the experimental spectra.

The RAS spectrum of the quenched (4×2) has one broad minimum at low photon energies and no other pronounced features. This may indicate partial surface disorder, possibly related to a quenched mobile surface species. Indications for that also come from X-ray diffraction studies [14], RHEED rocking curves [22], and total-energy calculations [37], where some disorder of the Ga adatoms were found. The main features of the optical anisotropy measured for (4×2) surfaces are reproduced by our calculations for the $\zeta(4 \times 2)$ model, indicating that this energetically favoured surface structure indeed explains the appearance of (4×2) symmetries for Ga-rich GaAs surfaces. The deviations between measured and calculated RAS spectra for the (4×2) surface are most likely related to the temperature and the above mentioned surface defects, in particular Ga adatoms.

From all the calculated (2×6) structures, only the mixed-dimer structure gives rise to a pronounced RAS minimum for a photon energy of about 2 eV as observed experimentally for structures with six-fold symmetry along the $[110]$ direction. While the mixed-dimer (2×6) structure is energetically unfavorable, this may indicate that mixed dimers are nevertheless an essential building block for $n \times 6$ reconstructions.

One might think that the (4×6) surface is a superposition of $(2 \times 6)/(3 \times 6)$ and (4×2) reconstructed domains. However, the amplitude of the (4×6) RAS signal around 2 eV and in the UV range above 3.5 eV exceeds those of the $(2 \times 6)/(3 \times 6)$ and (4×2) reconstructions. Since the RAS signal is the linear combination of the contributions of the different surface domains, our data clearly show that the (4×6) is not a mixture of $(2 \times 6)/(3 \times 6)$ and (4×2) reconstructed domains, but rather a genuine reconstruction, most likely identical to the so-called G (4×6) surface discussed by Xue et al. [5, 11]. They proposed a regular array of Ga clusters containing 6 to 8 atoms on top of a (4×2) reconstructed GaAs surface to explain the structure of the (4×6) surface. This was based on bright protrusions seen in STM images [5, 11, 13]. But total-energy calculations [20, 37] found this cluster model to be unstable. Kruse et al. proposed that electrons in surface localized states of the (4×2) surface, so-called ghost states, are responsible for the (4×6) reconstruction [13]. However, such ghost states should give rise to additional features in the RAS spectra. However, no indication for that is found in the RAS spectra of (4×2) and (4×6) surfaces shown in Fig. 4.

By careful annealing near 800 K another (4×6) pattern shows up just before the (4×2) symmetry appears. Time-dependent RAS measurements at 2.0 eV and 4.5 eV show a continuous transition. This indicates that this pattern does not correspond to a single surface phase, but most likely to a mixture of $(2 \times 6)/(3 \times 6)$ and (4×2) reconstructed domains, i.e., the so-called pseudo or P (4×6) surface discussed in Ref. [11]. Its appearance might be due to slight temperature differences on the sample holder.

To conclude, we found three different stable structures on gallium-rich GaAs(001) surfaces, namely a $(2 \times 6)/(3 \times 6)$, a (4×2) , and a (4×6) reconstruction. The total-energy calculations and the comparison of measured and calculated optical anisotropy supports the ζ structure for (4×2) reconstructed surfaces. In the experiment we find this surface to be stable only above 800 K. A $(2 \times 6)/(3 \times 6)$ or, after offering Ga, a (4×6) reconstruction is formed below 800 K. The $(n \times 6)$ reconstructions cannot

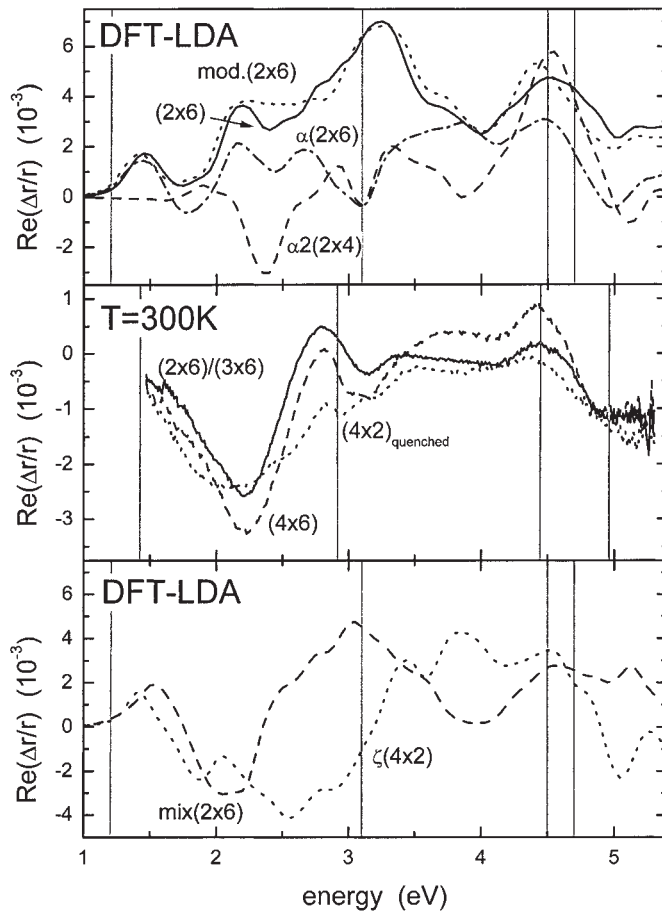


Fig. 4 RAS spectra $\text{Re}(r_{[1\bar{1}0]} - r_{[110]}/\langle r \rangle)$ measured at 300 K b) are compared with calculations a) and c). The calculated spectra in the upper Fig. a) disagree with the experimental findings or have a completely different shape. Gray vertical lines indicate the experimental/computational positions of the E_0 , E_1 , E'_0 , and E_2 critical points taken directly from the calculations or for the experiment from Ref. [36].

be explained by previously suggested (2×6) structures [7, 12, 29] because the suggested structures are energetically only metastable and their calculated RAS spectra do not agree with experiment. Furthermore, these models are not as gallium-rich as expected from the preparation conditions leading to six-fold symmetries. Replacement of top As dimers by mixed Ga-As dimers renders the surface more Ga-rich and leads to a much better agreement of the calculated RAS spectrum with experiment, suggesting mixed-dimers as a possibly building block of $(n \times 6)$ reconstructed surfaces.

Part of this work was performed through Special Coordination Funds of the Ministry of Education, Culture, Sports, Science, and Technology of the Japanese Government and by a grant of the Japanese Society for the Promotion of Science (JSPS). We gratefully acknowledge support by ONR and grants of computer time provided by the DoD Challenge Program, the Leibniz-Rechenzentrum München, the Höchstleistungsrechenzentrum Stuttgart, and the John von Neumann-Institut Jülich.

References

- [1] A. Cho, *J. Appl. Phys.* **47**, 2841 (1976).
- [2] A. J. van Bommel, J. E. Crombeen, and T. G. J. van Oirschot, *Surf. Sci.* **72**, 95 (1978).
- [3] C. W. Snyder, J. Sudijono, C.-H. Lam, M. D. Johnson, and B. G. Orr, *Phys. Rev. B* **50**, 18194 (1995).
- [4] J. Behrenda, M. Wassermeier, L. Däweritz, and K. H. Ploog, *Surf. Sci.* **342**, 63 (1995).
- [5] Q.-K. Xue, T. Hashizume, J. M. Zhou, T. Sakata, T. Ohno, and T. Sakurai, *Phys. Rev. Lett.* **74**, 3177 (1995).
- [6] Q.-K. Xue, T. Ogino, Y. Hasagawa, H. Shinohara, and T. Sakurai, *Phys. Rev. B* **53**, 1985 (1996).
- [7] D. K. Biegelsen, R. D. Bringans, J. E. Northrup, and L.-E. Swartz, *Phys. Rev. B* **41**, 5701 (1990).

- [8] I. Kamiya, D. E. Aspnes, L. T. Florez, and J. P. Harbison, *Phys. Rev. B* **46**, 15894 (1992).
- [9] D. W. Kisker, G. B. Stephenson, I. Kamiya, P. H. Fuoss, D. E. Aspnes, L. Mantese, and S. Brennan, *phys. stat. sol. (a)* **152**, 9 (1995).
- [10] I. Kamiya, L. Mantese, D. E. Aspnes, D. W. Kisker, P. H. Fuoss, G. B. Stephenson, and S. Brennan, *J. Cryst. Growth* **163**, 67 (1996).
- [11] Q.-K. Xue, T. Hashizume, and T. Sakurai, *Prog. Surf. Sci.* **56**, 1 (1997).
- [12] J. G. McLean, P. Kruse, and A. C. Kummel, *Surf. Sci.* **424**, 206 (1999).
- [13] P. Kruse, J. G. McLean, and A. C. Kummel, *J. Chem. Phys.* **113**, 2060 (2000).
- [14] C. Kumpf, L. D. Marks, D. Ellis, D. Smilgies, E. Landemark, M. Nielsen, R. Feidenhans'l, J. Zegenhagen, O. Bunk, J. H. Zeysing, Y. Su, and R. L. Johnson, *Phys. Rev. Lett.* **86**, 3586 (2001).
- [15] N. Esser, W. G. Schmidt, C. Cobet, K. Fleischer, A. I. Shkrebtii, B. O. Fimland, and W. Richter, *J. Vac. Sci. Technol. B* **19**, 1756 (2001).
- [16] D. Paget, Y. Garreau, M. Sauvage, P. Chiaradia, R. Pinchaux, and W. G. Schmidt, *Phys. Rev. B* **64**, R161305 (2001).
- [17] S. B. Zhang and A. Zunger, *Phys. Rev. B* **53**, 1343 (1996).
- [18] S.-H. Lee, W. Moritz, and M. Scheffler, *Phys. Rev. Lett.* **85**, 3890 (2000).
- [19] W. G. Schmidt, S. Mirbt, and F. Bechstedt, *Phys. Rev. B* **62**, 8087 (2000).
- [20] W. G. Schmidt, *Appl. Phys. A* **75** (2002) 89.
- [21] S. Tsukamoto, M. Pristovsek, A. Ohtake, B. G. Orr, G. R. Bell, T. Ohno, and N. Koguchi, *J. Cryst. Growth* **251**, 46 (2003).
- [22] A. Ohtake, S. Tsukamoto, M. Pristovsek, N. Koguchi, and M. Ozeki, *Phys. Rev. B* **65**, 233311 (2002).
- [23] E. L. Briggs, D. J. Sullivan, and J. Bernholc, *Phys. Rev. B* **54**, 14362 (1996).
- [24] R. Del Sole, *Solid State Commun.* **37**, 537 (1981).
- [25] F. Manghi, R. Del Sole, A. Selloni, and E. Molinari, *Phys. Rev. B* **41**, 9935 (1990).
- [26] P. H. Hahn, W. G. Schmidt, and F. Bechstedt, *Phys. Rev. Lett.* **88**, 016402 (2002).
- [27] W. G. Schmidt, F. Bechstedt, and J. Bernholc, *J. Vac. Sci. Technol. B* **18**, 2215 (2000).
- [28] R. Del Sole and R. Girlanda, *Phys. Rev. B* **48**, 11789 (1993).
- [29] M. Kuball, D. Wang, N. Esser, M. Cardona, J. Zegenhagen, and B. Fimland, *Phys. Rev. B* **51**, 13880 (1995).
- [30] C. Ratsch, *Phys. Rev. B* **63**, R161306 (2001).
- [31] A. Kley, Dr. Thesis, Technische Universität Berlin, Germany (1997).
- [32] C. R. Bayliss and D. L. Kirk, *J. Phys. D* **9**, 233 (1976).
- [33] C. Sasaoka, Y. Kato, and A. Usui, *Surf. Sci. Lett.* **265**, L239 (1992).
- [34] B. A. Banse and J. R. Creighton, *Mater. Res. Soc. Symp. Proc.* **222**, 15 (1991).
- [35] W. Mönch, *Semiconductor Surfaces and Interfaces*, 3rd ed. (Springer-Verlag, Berlin, 2001).
- [36] P. Lautenschlager, M. Garriga, S. Logothetidis, and M. Cardona, *Phys. Rev. B* **35**, 9174 (1987).
- [37] K. Seino, W. G. Schmidt, F. Bechstedt, and J. Bernholc, *Surf. Sci.* **507**, 406 (2002).